

# Synthesis and characterisation of novel flame retardant polyurethanes containing designed phosphorus units

Shih-Hsuan Chiu<sup>1</sup> · Cheng-Lung Wu<sup>1</sup> · Hsun-Tsing Lee<sup>2</sup> · Jia-Hao Gu<sup>1</sup> · Maw-Cherng Suen<sup>3</sup>

Received: 22 March 2016 / Accepted: 23 August 2016 / Published online: 6 September 2016  
© Springer Science+Business Media Dordrecht 2016

**Abstract** In this study, 2-carboxyethyl(phenyl)phosphinic acid (CEPPA) and trimethylolpropane (TMP) are used to synthesise a novel flame retardant containing phosphorus units: 5-hydroxy-3-(2-hydroxyethyl)-3-methylpentyl-3-[2-carboxyethylphenylphosphine]propanoate (HMCPP). Then, 4,4'-diphenylmethane diisocyanate (MDI) is taken as a hard segment, with HMCPP and polycaprolactone diol (PCL) as soft segments, and 1,4-butanediol (BD) is used as a chain extender to prepare a novel polyurethane (HMCPP/PUs). The results of <sup>1</sup>H NMR and FT-IR reveal the successful synthesis of the HMCPP flame retardant. The gel permeation chromatography analysis demonstrates that an increase in the HMCPP content is accompanied by a decrease in the molecular weight of PU. The FT-IR analysis reveals the complete NCO group exhaustion of PU and HMCPP/PUs. The thermal analysis shows that the initial decomposition temperature of PU is higher than that of HMCPP/PUs by 19 °C. Both DMA and DSC analyses show that the T<sub>g</sub> and the dynamic T<sub>g</sub> of PU are higher than those of HMCPP/PU. Stress-strain tests indicate that the HMCPP content is increased, the maximum stress and Young's modulus of HMCPP/PUs are decreased, and the elongation at break is increased. All of the HMCPP/PUs exhibit excellent flame retardancy,

obtaining higher than 27.7 in limiting oxygen indices and a V-0 rating in the UL-94 test.

**Keywords** Polyurethane · Phosphorus · Flame retardant · Chain extender

## Introduction

Polyurethane (PU) is a multi-functional elastomer. It may be used to synthesise materials with different properties by changing the proportions of soft segments and hard segments. Because of this characteristic, PU is widely applied in the flooring surfaces of indoor stadia, sneaker materials, waterproofing agents for buildings, foam plastics, and coatings, and therefore, it holds an important position in the industrial field [1–5].

In recent years, the excessive application of conventional resins has caused a multitude of problems, including environmental pollution and the rapid depletion of petroleum as a source of energy. Therefore, the need for renewable resources and the development of biodegradable polymers has become an important research task [6–8]. Biodegradable polyurethanes are often synthesised using soft segments that are easily hydrolysed. Generally, they are biocompatible, have low crystallinity and a low melting point, or are water-soluble [9–13]. Meanwhile, biodegradable PUs still retain excellent physical properties and biocompatibility and are able to reduce the production of waste, which is why many researchers are actively studying them [14, 15].

Because of the increasing demand for polymers, developing safe flame-retarding polymers is imperative. By definition, a flame retardant may retard the combustion of polymers through retarding or inhibiting the thermal decomposition or oxidation of polymers by means of chemical compounds. Flame retardants may be applied in consumer products by

✉ Maw-Cherng Suen  
sun@tiit.edu.tw

<sup>1</sup> Department of Materials Science and Engineering, National Taiwan University of Science and Technology, Taipei, Taiwan 10607, Republic of China

<sup>2</sup> Department of Materials Science and Engineering, Vanung University, Jongli, Taoyuan, Taiwan 32061, Republic of China

<sup>3</sup> Department of Creative Fashion Design, Taoyuan Innovation Institute of Technology, No. 414, Sec. 3, Zhongshan E. Rd, Taoyuan, Taiwan 32091, Republic of China

physical or chemical methods [16, 17]. The majority of flame retardants contain phosphorus, antimony, aluminum, boron, chlorides, and bromides. The strongest merits of inorganic flame retardants are their low toxicity, low smoke production, and low corrosion. Moreover, they are cheap, but as they need to be added to products in larger quantities, the mechanical performance of materials is often affected, thus limiting their applications. Flame retardant containing phosphorus units is one of the three major types of flame retardant. At present, with such advantages as low smoke production, an absence of toxicity, and low or no halogen content, it has gradually increased in popularity as environmental protection requirements have become more stringent. Compounds containing phosphorus units may be used as polymer flame retardants [18–23]. For example, Liu et al. studied the synthesis of polyhydric alcohols containing phosphorus units in the polymeric backbone, and the results demonstrated an increase in the flame-retarding properties of polymers [22]. The flame-retarding properties of PUs may be improved in two ways: by using additive-type flame retardants or by using reactive-type flame retardants. Using additive-type flame retardants is simple compared with using reactive-type flame retardants. However, by incorporating flame retardant containing chemical units into polymers, flame-retarding effects are achieved more effectively [24]. This is because the chief advantage of using reactive-type flame retardants lies in the fact that the polymers are endowed with a permanent flame-retarding performance while retaining their original physical properties. Therefore, many scholars have focused on developing polymers whose backbone contains phosphorus [25–27].

In this paper, we synthesise a novel flame retardant containing phosphorus units (HMCPP). The synthesis of this novel flame retardant is achieved through the esterification of 2-carboxyethyl(phenyl)phosphinic acid and trimethylolpropane. Thereafter, HMCPP is reacted with PCL and MDI to generate a prepolymer of PU, and then a 1,4-BD chain extender is added to produce the HMCPP/PUs polymers. The effects of the HMCPP segments and the BD chain extender on the structure, molecular weight, thermal properties, and mechanical properties of the polyurethanes are reported. The flammability of the polyurethanes was evaluated via UL-94 tests and LOI tests experiments.

## Experimental

### Materials

2-Carboxyethyl(phenyl)phosphinic acid (CEPPA) was purchased from I-TAI Chemicals Inc. Trimethylolpropane (TMP), polycaprolactone diol (PCL,  $M_w = 530$ ), 4,4'-diphenylmethane diisocyanate (MDI), 1,4-butanediol, N,N'-dicyclohexylcarbodiimide (DCC), and trifluoroacetic acid

(TFA) were obtained from Aldrich. Tetrahydrofuran (THF) and N,N-dimethylacetamide (DMAc) were purchased from Mallinckrodt Chemicals.

### Synthesis of HMCPP

First, CEPPA was dissolved in 80 ml of THF in a 500-ml flat-bottomed flask. Subsequently, TMP and DCC were added and dissolved in the CEPPA solution with a mole ratio of CEPPA/TMP of 1/1. To this solution, two drops of TFA were added as a catalyst. The reaction between CEPPA and TMP proceeded at 65 °C with stirring at 300 rpm for 12 h. Then, the HMCPP was obtained using vacuum drying, and was subsequently dried in a 50 °C oven for 1 d.  $^{31}\text{P}$  NMR (DMSO- $d_6$ ): single peak at  $\delta = 34.6$  ppm.

### Synthesis of HMCPP/PUs

The materials of MDI, PCL, HMCPP, and DMAc were added to a 500-ml three-necked flask. Subsequently, the mixture was heated to 80 °C and stirred using a stirrer at 200 rpm. The PU prepolymer was formed 2 h after the reaction. The BD compound was added to mix with DMAc in the flask, and the reaction proceeded for 1 h (Scheme 2). The obtained HMCPP/PUs solution was poured into a serum bottle, and was stored in a refrigerator for 1 d. Finally, the HMCPP/PUs solution was poured onto a Teflon plate and was dried in a temperature-programmable circulating oven for 8 h. The formula and hard segment and soft segment contents of the HMCPP/PUs films are shown in Table 1. The hard segment and soft segment contents were calculated according to equations (2.1) and (2.2).

$$\begin{aligned} \text{Hard segment content (wt\%)} \\ = \frac{W_{MDI} + W_{BD}}{W_{MDI} + W_{PCL} + W_{HMCPP} + W_{BD}} \times 100\% \end{aligned} \quad (2.1)$$

$$\begin{aligned} \text{Soft segment content (wt\%)} \\ = 100\% - \text{Hard segment content (wt\%)} \end{aligned} \quad (2.2)$$

- $W_{MDI}$ : weight of MDI
- $W_{HMCPP}$ : weight of HMCPP
- $W_{PCL}$ : weight of PCL
- $W_{BD}$ : weight of BD

### $^1\text{H}$ NMR spectrometry

The  $^1\text{H}$  NMR (in DMSO- $d_6$ ) spectra of the specimens were measured using a Bruker Avance 300 spectrometer (300 MHz).

**Table 1** Formula of the HMCPP/PUs

Designation	MDI (moles)	PCL (moles)	HMCPP (moles)	1,4-BD (moles)	Hard segment (wt%)	Soft segment (wt%)
PU	4	3	-	1.0	36.36	63.64
HMCPP/PU-01	4	3	0.3	0.7	38.63	61.37
HMCPP/PU-02	4	3	0.6	0.4	36.69	63.31
HMCPP/PU-03	4	3	0.9	0.1	34.84	65.16

### Fourier transform infrared spectroscopy (FT-IR)

The Fourier transform infrared spectroscopy (FT-IR) was conducted on a PerkinElmer spectrometer (model Spectrum One). The spectra of the samples were obtained by scanning 16 times on average ranging from 4000 to 650  $\text{cm}^{-1}$  with a resolution of 2  $\text{cm}^{-1}$ .

### Gel permeation chromatography (GPC)

Gel permeation chromatography (GPC) was conducted using Analytical Scientific Instruments Model 500, which consisted of a refractive index (RI) detector (Schambeck RI2000) and two columns in a series of Jordi gel DVB mixed beds. A 10,000 Å bed at 30 °C was used to measure the molecular weight distribution relative to the polystyrene standards. The calibration was performed using eight standards, whose molecular weights ranging from 3420 to  $2.57 \times 10^6$ . The solvent was tetrahydrofuran at a flow rate of 1 mL/min.

### Thermogravimetric analysis (TGA)

A thermogravimetric analysis (TGA) was performed on a PerkinElmer TGA (model Pyris 1). The samples weighed 5–8 mg and were heated from room temperature to 700 °C in a nitrogen atmosphere at a heating rate of 10 °C/min.

### Differential scanning calorimetry (DSC)

Differential scanning calorimetry (DSC) was performed on a PerkinElmer DSC (model Jade). The samples were sealed in aluminum pans. The scans were subsequently performed in a nitrogen atmosphere. The scanning temperature ranged from –50 °C to 50 °C, and the heating rate was 10 °C/min. The glass transition temperatures ( $T_g$ ) were recorded at the mid-points of the curve slope. The total weights of the samples were 5–8 mg.

### Dynamic mechanical analysis (DMA)

A dynamic mechanical analysis (DMA) was performed on a SEIKO DMS (model SII Muse, DMS6100). The DMA was conducted in the tension mode with the frequency of 1 Hz and

a 5- $\mu\text{m}$  amplitude. The temperature ranged from –50 °C to 50 °C, and the heating rate was 3 °C/min. The specimen dimensions were 20 × 5 × 0.2 mm (L × W × H). The  $T_g$  was determined as the peak temperature of the glass transition region in the  $\tan \delta$  curve.

### Stress strain testing

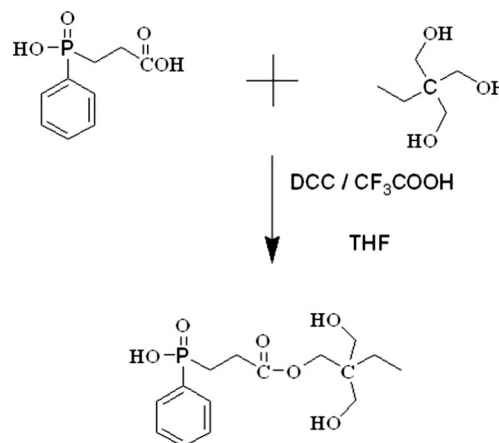
A universal testing machine (MTS QTEST5, model QC505B1) was used to measure the tensile strength and elongation at the break. The testing was conducted according to ASTM D638. The dimensions of the film specimen were 45 × 8 × 0.2 mm.

### Energy-dispersive X-ray spectroscopy (EDS) observations

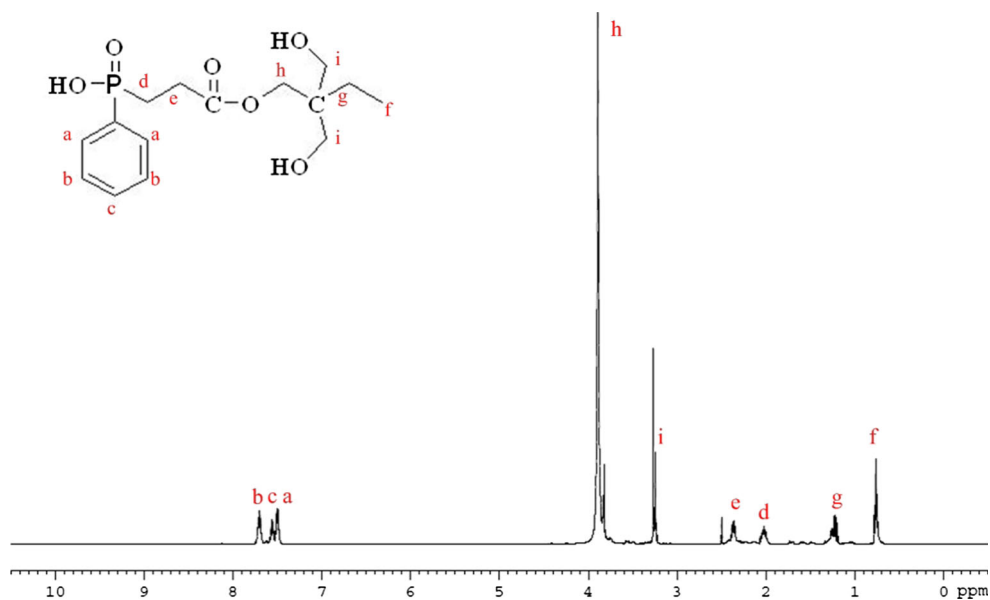
Energy dispersive X-ray spectroscopy (Bruker model XFlash 6|10) was used to examine the chemical composition of the HMCPP/PUs. The samples were 2 × 2  $\text{cm}^2$  in size and were fixed onto a sample holder by using conductive adhesive tape, and were coated with a thin layer of gold. The samples were photographed at 1 K magnification.

### X-ray photoelectron spectroscopy

X-ray photoelectron spectroscopy (XPS) was performed using a Thermo Fisher Scientific spectrometer. An Al  $K\alpha$  anode was used as the X-ray source (1486.6 eV),

**Scheme 1** Reaction formula for the HMCPP

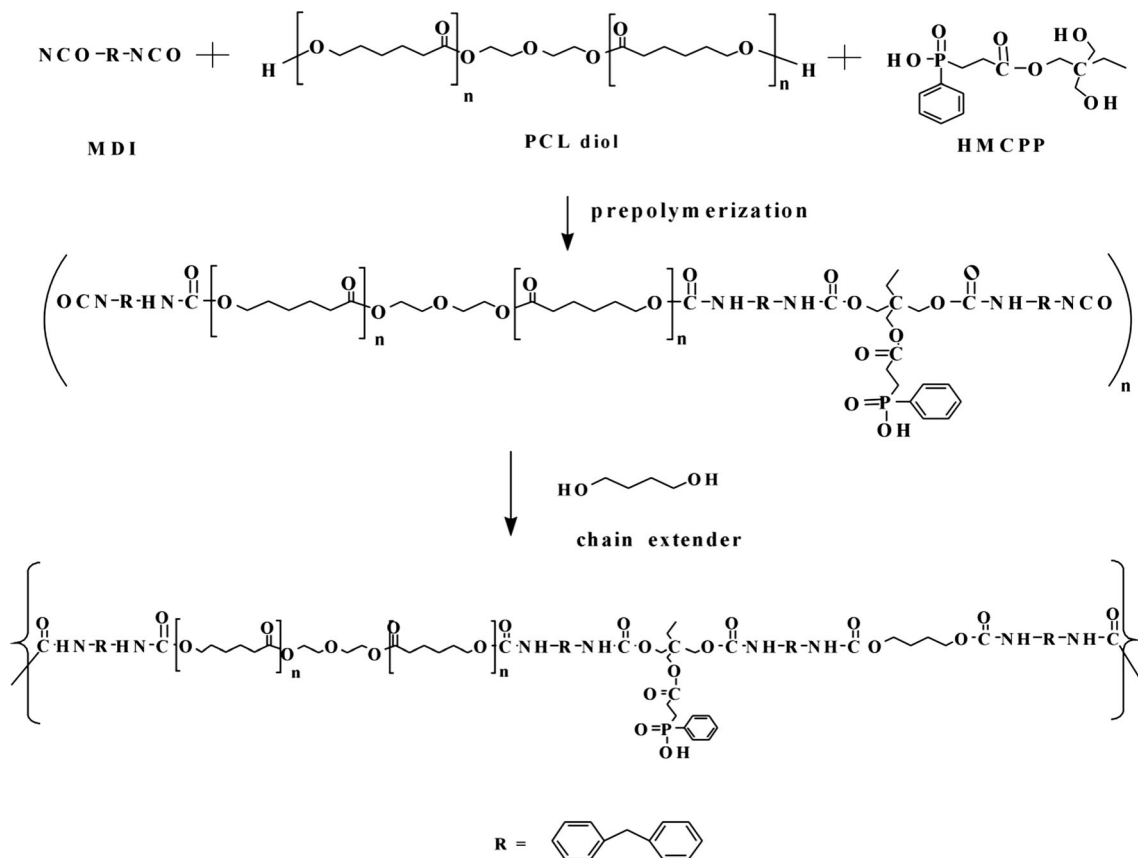
**Fig. 1**  $^1\text{H}$ NMR spectra of the HMCPP



and a binding energy range from 0 to 1400 eV was selected for analysis. The binding energies were calibrated to the C 1 s internal standard with a peak at 284.8 eV. The high-resolution C 1 s spectra were decomposed by fitting a Gaussian function to an experimental curve by using a nonlinear regression.

### LOI test

The limiting oxygen indices (LOI) were measured on a CSI oxygen index meter (Atlas). The dimensions of the specimen were  $140 \times 52 \times 0.3$  mm, and the height of the flame was 6–25 mm, in accordance with ASTM D2863.



**Scheme 2** HMCPP/PUs reaction formula

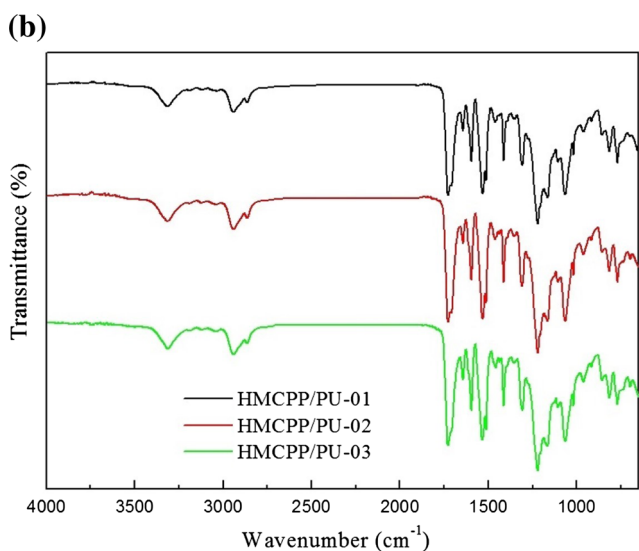
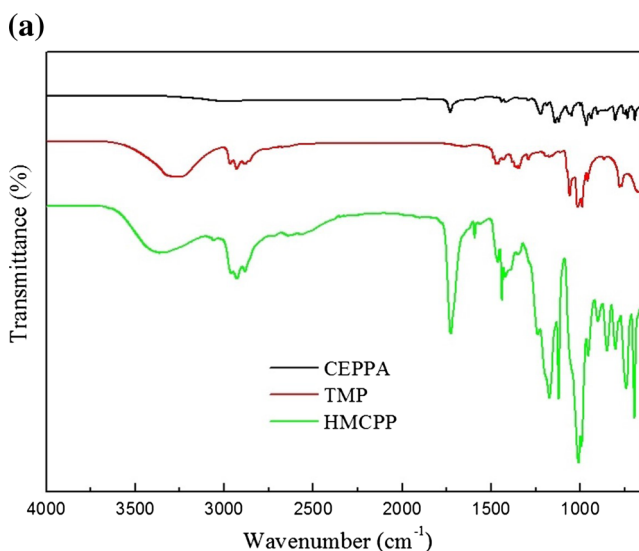


**Fig. 2** FTIR spectra of the (a) HMCPP and (b) HMCPP/PUs

### UL-94 test

Vertical burning measurements were conducted with a vertical burning test instrument (VC-1) (Govmark) with specimen dimensions of  $200 \times 50$  mm, in accordance with ASTM D3801.

## Results and discussion

### $^1\text{H}$ NMR

The reaction formula for HMCPP is shown in Scheme 1.  $^1\text{H}$  NMR (DMSO- $d_6$ , Fig. 1)  $\delta$  ppm: a: 7.48 (m, 2H, aromatic Ha), b: 7.70 (m, 2H, aromatic Hb), c: 7.56 (m, 1H, aromatic Hc), d: 2.02 (m, 2H,  $\text{CH}_2$  Hd), e: 2.36 (m, 2H,  $\text{CH}_2$  He), f: 0.75 (m, 3H,  $\text{CH}_3$ , Hf), g: 1.25 (m, 2H,  $\text{CH}_2$ , Hg), h: 3.83 (d, 2H,  $\text{CH}_2$ , Hh), i: 3.24 (d, 4H,  $\text{CH}_2$ , Hi) (Scheme 2).

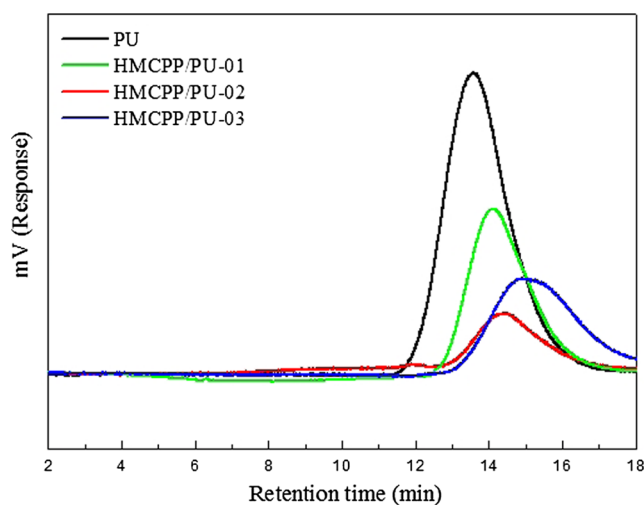


**Fig. 3** GPC curves of HMCPP/PUs

### Fourier transform infrared spectroscopy (FT-IR)

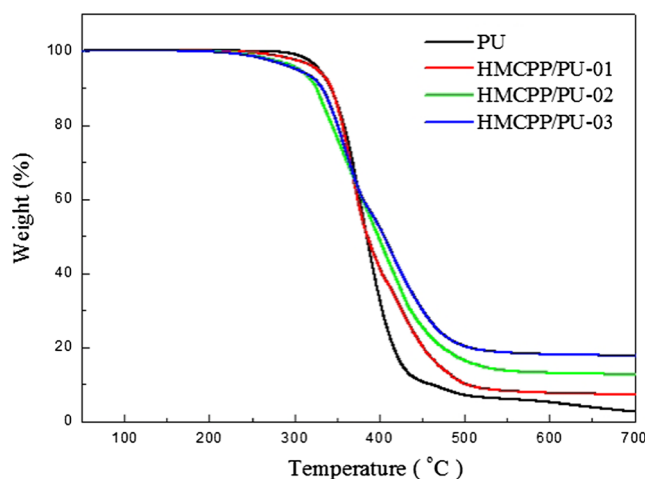
The FT-IR spectrum of HMCPP is shown in Fig. 2a. As shown in the spectrum, the hydroxyl group ( $-\text{OH}$ ), as the major absorption peak of HMCPP, appeared at  $3364\text{ cm}^{-1}$ . The symmetrical and asymmetrical stretching vibration peaks of  $\text{CH}_2$  appeared at  $2938\text{ cm}^{-1}$  and  $2884\text{ cm}^{-1}$ . The appearance of these absorption peaks is attributed to TMP. The formation of the HMCPP structure was revealed by the peak observed at  $1729\text{ cm}^{-1}$  for the carbonyl group ( $\text{C}=\text{O}$ ), the peak near  $1594\text{ cm}^{-1}$ , which denotes the  $\text{C}=\text{C}$  resonance absorption peak of the benzene ring, the peak at  $1185\text{ cm}^{-1}$  ( $\text{P}=\text{O}$  stretching), and the one at  $1438\text{ cm}^{-1}$  ( $\text{P}-\text{Ph}$  stretching) [28], as well as the  $\text{C}-\text{O}$  stretching vibration peak at  $1216\text{ cm}^{-1}$ . Figures 1 and 2a verify that the HMCPP flame retardant was successfully synthesised in this study.

Figure 2b presents the FT-IR spectra of PU and HMCPP/PUs in a wavenumber range of  $4000$  to  $650\text{ cm}^{-1}$ . There are five main common peaks in the spectra of all of these polymers. That is, the  $-\text{NH}$  stretching vibration peak appears at  $3315\text{ cm}^{-1}$ , the peaks at  $2941\text{ cm}^{-1}$  and  $2863\text{ cm}^{-1}$  are the stretching vibrations of  $\text{CH}_2$ , and the peak near  $1729\text{ cm}^{-1}$  represents carbonyl group ( $\text{C}=\text{O}$ ). The peak at  $1531\text{ cm}^{-1}$  is due to the  $\text{NH}$  vibration of the associated secondary urethane groups. The peaks at  $1643$  and  $1595\text{ cm}^{-1}$  are due to the  $\text{C}=\text{C}$  stretching vibration. The  $\text{C}-\text{O}$  stretching vibration peak

**Table 2** GPC results of HMCPP/PUs

	Retention time of the peak (min)	$\overline{Mn}$ ( $\times 10^4$ )	$\overline{Mw}$ ( $\times 10^4$ )	$\overline{Mw}/\overline{Mn}$
PU	13.6	5.01	6.92	1.5
HMCPP/PU-01	14.0	3.56	5.39	1.5
HMCPP/PU-02	14.4	2.70	4.38	1.7
HMCPP/PU-03	15.1	1.96	3.51	1.8





**Fig. 4** TGA curves of the HMCPP/PUs

appears near  $1217\text{ cm}^{-1}$ . Moreover, no peak of the free NCO group at  $2240\text{--}2275\text{ cm}^{-1}$  is observed in these spectra. Therefore, the MDI was fully reacted with the PCL, HMCPP and 1,4-BD chain extender during the synthesis process

### Gel permeation chromatography analysis

Figure 3 depicts the GPC curves of the PU synthesized with different proportions of HMCPP. For these polymers, the distribution of molecular weight is unimodal, and no residual starting material remains in these samples. The calculated Mw and Mn are recorded in Table 2. The molecular weight of PU decreases along with an increase in the HMCPP content. The Mw/Mn values, i.e., the broadness of the molecular weight distributions, are in the range of 1.5 to 1.8. The molecular weight distribution of PU broadens along with an increase in HMCPP content. During the synthesis process, the viscosity of the polymer solution decreases with an increase in the HMCPP content. In other words, reducing the chain extender content lowers the PU molecular weight.

### Thermal properties

Figure 4 presents the TGA curves of PU with different proportions of HMCPP. The decomposition temperature

**Table 3** Thermal properties of the HMCPP/PUs

Sample	TGA T <sub>onset</sub> (°C)	Residue at 700 °C (%)	DSC T <sub>g</sub> (°C)
PU	344.9	2.67	6.0
HMCPP/PU-01	340.7	7.29	3.6
HMCPP/PU-02	330.9	12.73	-0.6
HMCPP/PU-03	325.7	17.71	-7.8

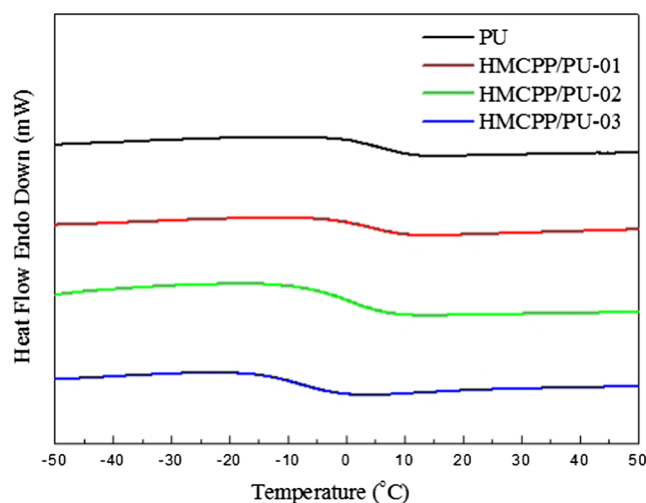


**Fig. 5** DSC thermograms of the HMCPP/PUs

corresponds to the urethane group. The onset temperatures, namely, the initial decomposition temperatures of HMCPP/PUs, are listed in Table 3. The initial decomposition temperatures of PU, HMCPP/PU-01, HMCPP/PU-02, and HMCPP/PUs-03 are 344.9, 340.7, 330.9, and 325.7 °C, respectively.

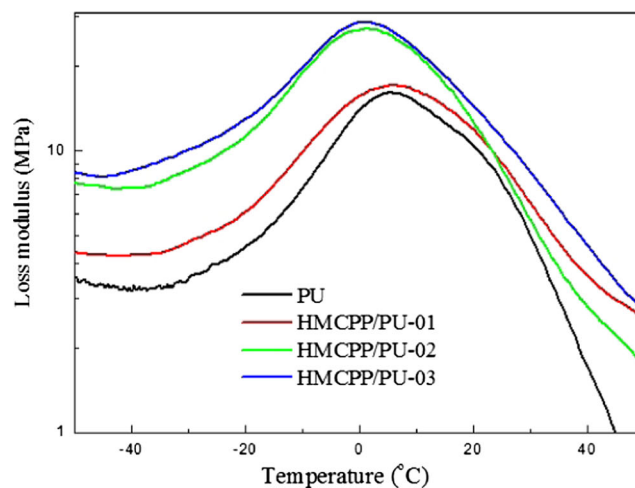
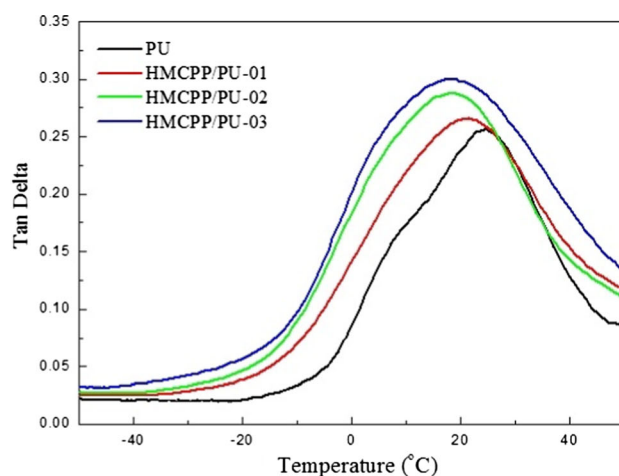


**Fig. 6** Tan  $\delta$  and loss modulus ( $E''$ ) curves of the HMCPP/PUs

**Table 4** DMA results of the HMCPP/PUs

Sample	$T_{gd}$ from $\tan\delta$ ( $^{\circ}\text{C}$ )	$\tan\delta_{\max}$	$T_{gd}$ from $E''$ ( $^{\circ}\text{C}$ )	$E''_{\max}$ (MPa)
PU	24.63	0.2561	5.7	15.98
HMCPP/PU-01	21.6	0.2655	3.4	17.16
HMCPP/PU-02	18.4	0.2887	0.8	27.29
HMCPP/PU-03	17.2	0.3010	0.1	28.90

The data in Table 3 indicate that the initial decomposition temperatures of PU was 344.9  $^{\circ}\text{C}$ , decreasing to 325.7  $^{\circ}\text{C}$  as the ratio of HMCPP increased to that of HMCPP/PU-03. This phenomenon may be attributed to the following two factors. First, the bonding energy of the P-O bond (149 kJ/mol) in the backbone of these polymers is lower than that of the C = O bond (799 kJ/mol) [29]. Second, among the four PUs, HMCPP/PU-03 has the lowest chain extender content, and the content of hard segments decreases along with the chain extender content. In general, increasing the content of the hard segments will affect the PU thermal stability. Hence this phenomenon suggests that the thermal stability of PU will be reduced with a decrease in the content of the hard segments or the chain extender.

Figure 5 depicts the DSC thermograms of the PU polymers with various HMCPP contents. This figure shows that all of the HMCPP/PUs display a single  $T_g$ , suggesting that the soft and hard segments of HMCPP/PUs are in the homogeneous phase [30]. The  $T_g$  values of PU, HMCPP/PU-01, HMCPP/PU-02, and HMCPP/PU-03 are 6.0, 3.6  $^{\circ}\text{C}$ ,  $-0.6$   $^{\circ}\text{C}$ , and  $-7.8$   $^{\circ}\text{C}$ , respectively. These  $T_g$  values are also recorded in Table 3. This result indicates that an increase in the HMCPP content decreases the  $T_g$  of PU. This phenomenon may be because the HMCPP bulky pendant groups in the PU backbone lead to an increase in the free volume of the polymer chains so that the polymer chains are more labile for segmental motion. In addition,  $T_g$  is reduced with a decrease in the BD content. This is because the BD chain extender is a hard

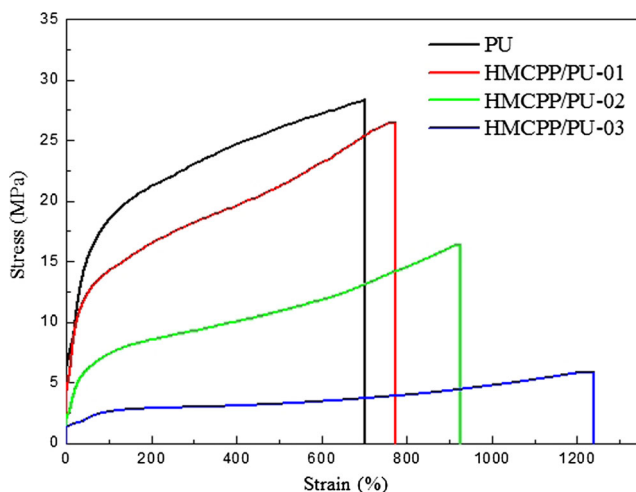
segment and reducing hard segments will lower  $T_g$ . This result is consistent with the TGA result. Decreasing the content of the BD chain extender or the hard segments will lower the thermal stability of PU.

### Dynamic mechanical analysis (DMA)

Figure 6 shows the  $\tan\delta$  and loss modulus curves of the PU with various HMCPP contents. The dynamic glass transition temperatures ( $T_{gd}$ ) were typically located at  $\tan\delta$  or  $E''$  curves. From the  $\tan\delta$  curves, the dynamic glass transition temperatures ( $T_{gd}$ ) of PU, HMCPP/PU-01, HMCPP/PU-02, and HMCPP/PU-03 are 24.63, 21.6, 18.4, and 17.2  $^{\circ}\text{C}$ , respectively. Conversely, the  $T_{gd}$  values from the  $E''$  curves are around 3–0  $^{\circ}\text{C}$  lower than the  $T_{gd}$  values from the  $\tan\delta$  curves. Therefore, the use of different testing methods will produce different  $T_g$  values. The results are recorded in Table 4. The dynamic glass transition temperatures of PU are lowered with an increase in the HMCPP content. This result is consistent with the aforementioned DSC result. Additionally, in  $\tan\delta$  or  $E''$  curves, the height of the  $T_{gd}$  peak with more HMCPP is higher than that with less HMCPP. This is because increasing the HMCPP content will lower the content of the BD chain extender, leading to an increase in the polymer viscosity and a decrease in the polymer elasticity. Therefore, increasing the HMCPP content will lead to a higher loss modulus. The loss modulus divided by the storage modulus equals  $\tan\delta$ . Therefore, HMCPP/PU-03, with the highest HMCPP content, exhibits the largest peak among the PU and three HMCPP/PUs. This influence is caused by the BD chain extender content, which decreases the viscosity of the HMCPP/PUs that contains more BD chain extender.

### Tensile properties

The stress-strain curves for the PU polymers with different HMCPP contents are shown in Fig. 7. The maximum stresses of PU, HMCPP/PU-01, HMCPP/PU-02, HMCPP/PU-03 are 28.3, 26.48, 16.62, and 6.07 MPa, and the Young's moduli are 3.3, 3.17, 1.43, and 0.36 MPa, respectively. The results are recorded in Table 5. This result indicates that increasing the HMCPP content will lower the maximum stress and the Young's modulus. This may be because an increase in the HMCPP content and a decrease in the BD content will

**Fig. 7** Tensile properties of the HMCPP/PUs stress-strain curves

**Table 5** Mechanical properties of the HMCPP/PUs

Sample	Maximum stress (MPa)	Elongation at break (%)	Young's modulus (MPa)
PU	28.30	702	3.30
HMCPP/PU-01	26.48	772	3.17
HMCPP/PU-02	16.62	921	1.43
HMCPP/PU-03	6.07	1235	0.36

decrease the content of hard segments. In other words, an increase in the content of the hard segments or the chain extender is beneficial for the tensile strength of PU. Therefore, the key to enhancing the tensile strength of PU lies in the content of hard segments. In addition, the elongation at break of these three polymers are 702, 772, 921, and 1235 %, in sequence; they are also recorded in Table 5. This result suggests that the increase in HMCPP content and the decrease in the content of hard segments are beneficial for the sliding motions among polymer chains. Therefore, the elongation at break is increased, and the content of hard segments is decreased.

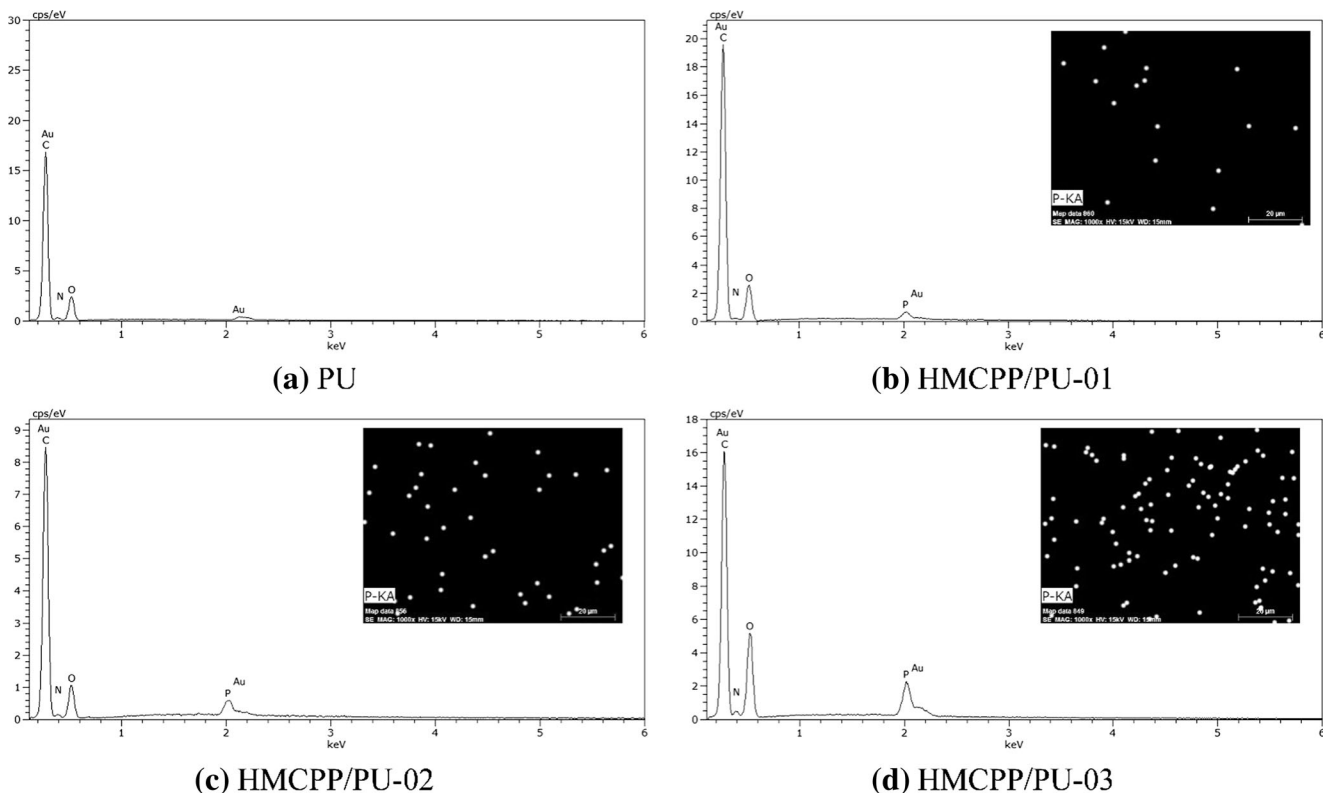
### Energy-dispersive X-ray spectroscopy (EDS)

Figure 8 shows the results of the elemental analysis from the energy dispersive X-ray spectra of the PU and HMCPP/PUs. The phosphorus content measured in PU, HMCPP/PU-01, HMCPP/PU-02, and HMCPP/PU-03 were 0 %, 1.36 %,

2.70 %, and 4.22 %, respectively. The phosphorus content increases with increasing HMCPP content, as is anticipated. The weight ratios of phosphorus are listed in Table 7. Mapping suggests that the distribution of elemental phosphorus is increased along with the increase in the HMCPP content.

### X-ray photoelectron spectroscopy (XPS)

The chemical composition and chemical state of the HMCPP/PU were determined using XPS. The XPS spectra of HMCPP/PUs are illustrated in Fig. 9. For HMCPP/PU-01, HMCPP/PU-02, and HMCPP/PU-03, each spectrum contains four major peaks corresponding to the four orbitals of C 1s, O 1s, N 1s, and P 1s. The elemental compositions and associated peak characteristics are recorded in Table 6. The binding energies of C 1s, N 1s, O 1s, and P 1s increase. This result is similar to the EDS analysis, the HMCPP content increased as the phosphorus content increased.

**Fig. 8** EDS images of the HMCPP/PUs



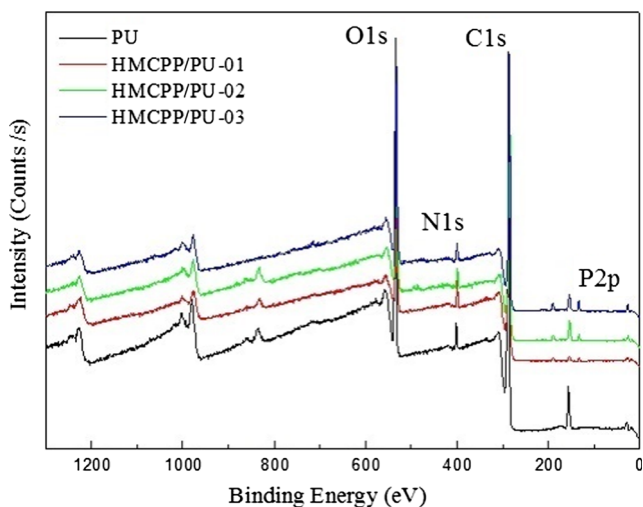


Fig. 9 XPS survey spectra of the HMCPP/PUs

**Flammability testing**

The LOI test and UL-94 test are widely applied for evaluating the flame-retarding performance of materials. Generally, an LOI value indicates the minimum concentration of oxygen required for the combustion of materials. The UL-94 test is generally used to determine the ignition and flame spread of materials. The results of this test are classified as flammability ratings V-0, V-1, and V-2. The V-0 rating is the highest flame retardant rating. This rating indicates the flame can neither spread upwards nor drip, whereas the V-1 and V-2 ratings indicate the possibility of nonflaming and flaming drips, respectively. Table 7 presents the LOI values of the flame-retarding PU and HMCPP/PUs. All of the HMCPP/PUs studied in this paper attain the UL94 V-0 rating. When HMCPP is exposed to fire, a char layer that does not easily combust will form on the polymer surface. This char layer serves as an effective shield and insulation for the polymer. It is able to prevent the underlying materials from being exposed to oxygen and flame. The structure and formation of this char layer is attributed to the HMCPP flame retardant. Generally speaking, to achieve a level of flame retardancy, the LOI value must be at least 26 [31, 32]. From Table 7, it may be observed that the LOI values of HMCPP/PUs increase with an increase in the HMCPP content. For example, the LOI value of HMCPP/PU-01 is 27.7, and the LOI value of HMCPP/PU-03 is 31.8; hence, all of the samples manifest flame-retarding effects.

**Table 6** XPS data of the PU/HD and PU/OFHD

Sample	C (At.%)	N (At.%)	O (At.%)	P (At.%)
PU	76.02	2.36	21.62	-
HMCPP/PU-01	77.61	4.20	17.28	0.92
HMCPP/PU-02	73.24	3.52	21.85	1.38
HMCPP/PU-03	72.03	3.05	22.60	2.32

**Table 7** P content and flame retardancy of the HMCPP/PUs with various HMCPP contents

Sample	EDS P content (wt %)	LOI values	UL-94 rating	Drip
PU	0.00	21.0	V-2	Yes
HMCPP/PU-01	1.36	27.7	V-0	No
HMCPP/PU-02	2.70	29.2	V-0	No
HMCPP/PU-03	4.22	31.8	V-0	No

**Conclusions**

In this paper, we used 2-carboxyethyl(phenyl) phosphinic acid and trimethylolpropane to synthesise a novel HMCPP flame retardant. Simultaneously, HMCPP, PCL, and MDI were used to synthesise the PUs prepolymer, and then HMCPP/PUs polymers were produced by adding the BD chain extender. The structures of HMCPP and the HMCPP/PUs polymers were confirmed by the <sup>1</sup>H NMR and FT-IR spectra. The thermal analysis demonstrates that the initial decomposition temperatures, T<sub>g</sub> and T<sub>gd</sub>, of PU are lowered with an increase in the HMCPP content. This is attributed to two factors: First, the bulky pendant groups of HMCPP cause the polymer chains to be more labile for segmental motion, and the second factor is the increase in the HMCPP content and the decrease in the BD chain extender content. Maximum stresses and Young’s moduli of the PU samples decrease with increasing HMCPP content. In addition, along with an increase in the HMCPP content, HMCPP/PUs manifest excellent flame retardancy: higher than 27.7 in LOI and a V-0 rating in the UL-94 test.

**References**

1. Abraham GA, de Queiroz AAA, San Roman JS (2006) Hydrophilic hybrid IPNs of segmented polyurethanes and copolymers of vinylpyrrolidone for applications in medicine. *Biomaterials* 22: 1971–1985
2. Tien YI, Wei KH (2001) Hydrogen bonding and mechanical properties in segmented montmorillonite/polyurethane nanocomposites of different hard segment ratios. *Polymer* 42:3213–3221
3. Mequanint K, Sanderson R (2003) Nano-structure phosphorus-containing polyurethane dispersions: synthesis and crosslinking with melamine formaldehyde resin. *Polymer* 44:2631–2639
4. Gugliuzza A, Clarizia G, Golemme G, Drioli E (2002) New breathable and waterproof coatings for textiles: effect of an aliphatic polyurethane on the formation of PEEK-WC porous membranes. *Eur Polym J* 38:235–242
5. Park HB, Lee YM (2002) Separation of toluene/nitrogen through segmented polyurethane and polyurethane urea membranes with different soft segments. *J Membr Sci* 197:283–296
6. Gunatillake P, Mayadunne R, Adhikari R, El-Gewely MR (2006) Recent developments in biodegradable synthetic polymers. *Biotechnol Annu Rev* 12:301–347

7. Mohanty AK, Misra M, Drzal LT (2002) Sustainable biocomposites from renewable resources: opportunities and challenges in the green materials world. *J Polym Environ* 10:19–26
8. Mohanty AK, Misra M, Hinrichsen G (2000) Biofibres, biodegradable polymers and biocomposites: an overview. *Macromol Mater Eng* 276–277:1–24.
9. Chandra R, Rustgi R (1998) Biodegradable polymers. *Prog Polym Sci* 23:1273–1335
10. Okada M (2002) Chemical syntheses of biodegradable polymers. *Prog Polym Sci* 27:87–133
11. Nair LS, Laurencin CT (2007) Biodegradable polymers as biomaterials. *Prog Polym Sci* 32:762–798
12. Pena J, Corrales T, Izquierdo-Barba I, Doadrio AL, Vallet-Regi M (2006) Long term degradation of poly( $\epsilon$ -caprolactone) films in biologically related fluids. *Polym Degrad Stab* 91:1424–1432
13. Coulembier O, Degee P, Hedrick JL, Dubois P (2006) From controlled ring-opening polymerization to biodegradable aliphatic polyester: especially poly(b-malic acid) derivatives. *Prog Polym Sci* 31:723–747
14. Jiang X, Li JH, Ding MM, Tan H, Ling QY, Zhong YP (2007) Synthesis and degradation of nontoxic biodegradable waterborne polyurethanes elastomer with poly( $\epsilon$ -caprolactone) and poly(ethylene glycol) as soft segment. *Eur Polym J* 43:1838–1846
15. Tsou CH, Lee HT, Tsai HA, Cheng HJ, Suen MC (2013) Synthesis and properties of biodegradable polycaprolactone/polyurethanes by using 2,6-pyridinedimethanol as a chain extender. *Polym Degrad Stab* 98:643–650
16. Sain M, Park SH, Suhara F, Law S (2004) Flame retardant and mechanical properties of natural fibre-PP composites containing magnesium hydroxide. *Polym Degrad Stab* 83:363–367
17. Zhu S, Shi W (2003) Thermal degradation of a new flame retardant phosphate methacrylate polymer. *Polym Degrad Stab* 80:217–222
18. Liu YL, Hsiue CH, Lan CW, Kuo JK, Jeng RJ, Chiu YS (1997) Synthesis, thermal properties, and flame retardancy of phosphorus containing polyimides. *J Appl Polym Sci* 63:875–882
19. Yeh JT, Hsieh SH, Cheng YC, Yang MJ, Chen KN (1998) Combustion and smoke emission properties of poly(ethylene terephthalate) filled with phosphorous and metallic oxides. *Polym Degrad Stab* 61:399–407
20. Banks M, Ebdon JR, Johnson M (1994) The flame-retardant effect of diethylvinyl phosphonate in copolymers with styrene, methylmethacrylate, acrylonitrile and acrylamide. *Polymer* 35:3470–3474
21. Cheng TC, Chiu YS, Chen HB, Ho SY (1995) Degradation of phosphorus-containing polyurethanes. *Polym Degrad Stab* 47:375–381
22. Liu YL, Hsiue GH, Lee RH, Chiu YS (1997) Phosphorus-containing epoxy for flame retardant. III: using phosphorylated diamines as curing agents. *J Appl Polym Sci* 63:895–901
23. Zhao H, Wang YZ, Wang DY, Wu B, Chen DQ, Wang XL, Yang KK (2003) Kinetics of thermal degradation of flame retardant copolyesters containing phosphorus linked pendent groups. *Polym Degrad Stab* 80:135–140
24. Chen-Yang YW, Yuan CY, Li CH, Yang HC (2003) Preparation and characterization of novel flame retardant (aliphatic -phosphate)cyclotriphosphazene-containing polyurethanes. *J Appl Polym Sci* 90:1357–1364
25. Liu YL, Hsiue GH, Lan CW, Chiu YS (1997) Flame-retardant polyurethanes from phosphorus-containing isocyanates. *J Polym Sci A Polym Chem* 35:1769–1780
26. Chang TC, Chiu YS, Chen HB, Ho SY (1995) Degradation of phosphorus-containing polyurethanes. *Polym Degrad Stab* 47:375–381
27. Chang TC, Shen WY, Chiu YS, Ho SY (1995) Thermo-oxidative degradation of phosphorus-containing polyurethane. *Polym Degrad Stab* 49:353–360
28. Çelebi F, Polat O, Aras L, Güngör G, Akhmedov Idris M (2004) Synthesis and characterization of water-dispersed flame-retardant polyurethane resin using phosphorus-containing chain extender. *J Appl Polym Sci* 91:1314–1321
29. Huang WK, Yeh JT, Chen KJ, Chen KK (2001) Flame retardation improvement of aqueous-based polyurethane with aziridinyl phosphazene curing system. *J Appl Polym Sci* 79:662–673
30. Arun Prasath R, Nanjundan S, Pakula T, Klapper M (2004) Thermal and dynamic mechanical behaviour of calcium containing co-polyurethanes. *Polym Degrad Stab* 85:911–923
31. Cullis CF, Hirschler MM (1984) Char formation from Polyolefins. *Eur Polym J* 20:53–60
32. Wang DY, Liu Y, Wang YZ, Ariles CP, Hull TR, Price D (2007) Fire retardancy of a reactively extruded intumescent flame retardant polyethylene system enhanced by metal chelates. *Polym Degrad Stab* 92:1592–1598